ELSEVIER

Applied Surface Science 138–139 (1999) 212–217

applied surface science

Laser-induced thermal degradation and ablation of polymers: bulk model

N. Arnold [a,*], N. Bityurin [b], D. Bäuerle [a]

[a] *Angewandte Physik, Johannes-Kepler-Universität, Altenbergerstraße 69, A-4040, Linz, Austria*
[b] *Institute of Applied Physics RAS, Nizhnii Novgorod, Russian Federation*

Abstract

Ablation of organic polymers is described on the basis of *photothermal* bond breaking within the bulk material. Here, we assume a first order chemical reaction, which can be described by an Arrhenius law. Ablation starts when the density of broken bonds at the surface reaches a certain critical value. In order to understand the ablation behavior near the threshold fluence, ϕ_{th}, *non-stationary* regimes are considered. The present treatment reveals several qualitative differences with respect to models which treat ablation as a surface process: (i) Ablation starts sharply with a front velocity that has its maximum value just after the onset. (ii) The transition to quasi-stationary ablation is much faster. (iii) Near threshold, the ablated depth has a square-root dependence on laser fluence, $\phi - \phi_{th}$. (iv) With $\phi \approx \phi_{th}$, ablation starts well after the laser pulse. (v) The depletion of species is responsible for the Arrhenius tail with fluences $\phi \leq \phi_{th}$.

PACS: 82.65; 82.50; 42.10; 81.15Fg

Keywords: Laser ablation; Thermal degradation; Modeling; Polymers

1. Introduction

The physical mechanisms in UV–laser ablation of organic polymers are still under discussion [1,2]. The models proposed include *photochemical* [2–5], *photothermal*, and *photophysical* models [6]. Such models may be divided into *surface* models [7–9], and *volume* models. With volume models [10], the chemical process occurs within the bulk material. Previous investigations either considered heat conduction as a correction, or ignored the effect of the moving interface, which resulted in unrealistic temperatures (above 10^4 K) [11]. Consistent models should explain the sharp onset of ablation observed at $\phi \approx \phi_{th}$ in certain types of ablation rate measurements, the Arrhenius tail observed with $\phi \leq \phi_{th}$ in other types of experiments [12], and the dependence of the ablation rate on the repetition rate [13] and the duration of the laser pulse [9,14].

In the present article we shall apply the model introduced in Ref. [15] to *non-stationary* regimes and the description of the ablation process near the threshold.

* Corresponding author. Tel.: +43-732-2468-9245; Fax: +43-732-2468-9242; E-mail: nikita.arnold@jk.uni-linz.ac.at

0169-4332/99/$ - see front matter
PII: S0169-4332(98)00423-1

2. Model

A schematic picture of the model is shown in Fig. 1. The reference frame is fixed with the (moving) ablation front. For one-dimensional (1D) heat conduction, the heat equation can be written as

$$\frac{\partial H}{\partial t} = v\frac{\partial H}{\partial x} + \frac{\partial}{\partial x}\left(K\frac{\partial T}{\partial x}\right) - \frac{\partial I}{\partial x} \qquad (2.1)$$

Here, T is the temperature, K the thermal conductivity, and $I(x)$ the laser beam intensity which obeys Beer's law. T_0 is the ambient temperature, H the volumetric enthalpy, c the specific heat and ρ the density. First order thermally activated bond breaking *within* the material can be described by

$$\frac{\partial n_b}{\partial t} = v\frac{\partial n_b}{\partial x} + (1-n_b)\,k_0\exp(-T_a/T) \qquad (2.2)$$

Here, n_b is the fraction of bonds which are broken, $1-n_b$ the fraction of virgin bonds. k_0 is of the order of the IR vibrational frequency. The material decomposes when the number of broken bonds at the interface reaches a critical value, i.e. if

$$n_b|_{x=0} = n_{cr} \qquad (2.3)$$

The following boundary conditions are assumed:

$$-K\frac{\partial T}{\partial x}\bigg|_{x=0} = 0,\ T|_{x\to\infty} = T_0,\ n_b|_{x\to\infty} = 0 \qquad (2.4)$$

For *stationary* ablation, such a model is similar to surface thermal evaporation with re-normalized activation temperature and pre-exponential factor [15]. Stationary considerations, however, do not apply near ϕ_{th}, in particular for short pulses.

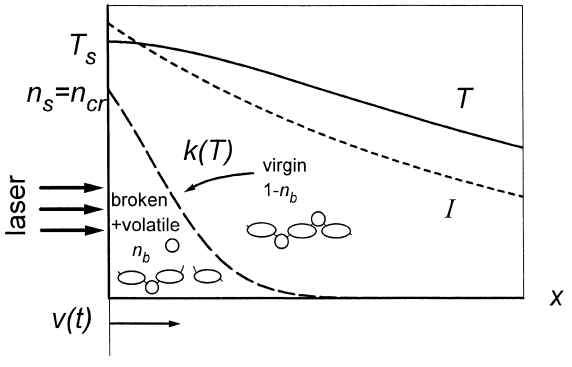

Fig. 1. Schematic of the model. The intensity I (dotted line) creates a temperature distribution T within the bulk material (solid line). Thermal bond breaking with a rate $k(T)$ takes place within the volume. It produces the distribution of broken bonds n_b (dashed line) and creates volatile species. The position of the interface is determined by the surface concentration $n_b(x=0) \equiv n_{cr}$.

3. Transient behavior

We now consider the transition to stationary ablation. It is convenient to rewrite Eq. (2.2) by introducing (positive) $b \equiv -\ln(1-n_b)$, which increases with n_b (the same holds for b_{cr} and n_{cr})

$$\frac{\partial b}{\partial t} = v\frac{\partial b}{\partial x} + k_0\exp(-T_a/T) \qquad (3.1)$$

We often employ the saddle point approximation for the reaction rate, which uses a Taylor expansion of T near the surface, under the assumption $T_a/T_s \gg 1$.

$$k_0\exp(-T_a/T) \approx k_s\exp\left(-x^2/l_k^2\right) \qquad (3.2)$$

$$k_s \equiv k_0\exp(-T_a/T_s),\ l_k \equiv (T_s/T_a)^{1/2},$$

$$l^2 \equiv -2T_s/\frac{\partial^2 T}{\partial x^2}\bigg|_{x=0} \qquad (3.3)$$

The index 's' refers to the surface $x=0$. l_k characterizes the width of the region, where the reaction takes place. l is the spatial width of the temperature distribution. Condition (2.4) allows to find $\partial^2 T/\partial x^2$ $(x=0)$ from the heat equation:

$$c_s\,\rho\dot{T}_s = K_s\frac{\partial^2 T}{\partial x^2}(x=0) + \alpha I_s \qquad (3.4)$$

Let us assume that n_{cr} (or b_{cr}) is reached at t_{cr} (Fig. 2). The solution of Eq. (3.1) for arbitrary $v(t)$ can be written with the help of the method of characteristics. Details of the derivation and the numerical procedure will be reported elsewhere [16]. Using

$$b|_{x=0}(t > t_{cr}) = \text{constant} \equiv b_{cr}, \qquad (3.5)$$

it is possible to obtain for the initial stage of ablation

$$h(t) = A(t-t_{cr})^{1/2},$$

$$A \approx \left[k_s(t_{cr})\Big/\int_0^{t_{cr}} k_s(t)\,dt\right]^{1/2} l_k(t_{cr}) \qquad (3.6)$$

The meaning of Eq. (3.6) is simple. Before ablation, the profile $n_b(x)$ is *parabolic* near $x=0$, because the temperature $T(x)$ and reaction rate $k(T(x))$ have

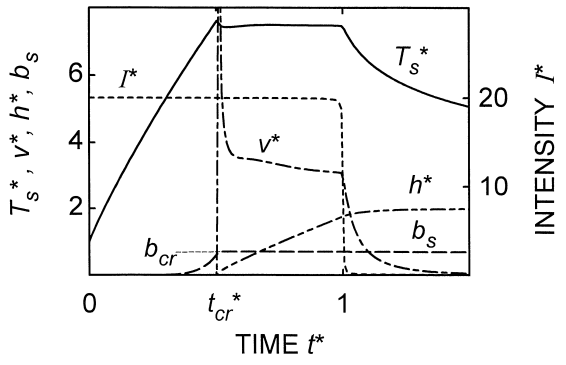

Fig. 2. Onset of ablation for $I=$ constant. Dotted curve at t_{cr}^* when b_{cr} is reached at the surface. The following dependences are included: Surface temperature T_s^* (solid), b_s (dashed), front velocity v^* (dash-dotted), ablated depth h^* (dash-double dotted). This figure, along with Fig. 3 and Fig. 4, uses dimensionless variables: $t^*=\alpha^2 Dt$, $h^*=\alpha h$, $v^*=v/\alpha D$, $T_s^*=T_s/T_0$, $I^*=I/\alpha KT_0$, $\phi^*=\phi\alpha/c\rho T_0$. Parameters in this figure, along with Fig. 3 and Fig. 4, satisfy the conditions: $A_s=1$, $\alpha^2 D\tau=1$, $k_0/D\alpha^2=10^5$, $T_a/T_0=70$, $n_{cr}=0.5$ ($b_{cr}=0.69$). They correspond, e.g., to $\tau=10$ ns, $D=10^{-2}$ cm^2/s, $\alpha=10^5$ cm^{-1}, $k_0=10^{13}$ s^{-1}, $T_a=21{,}000$ K $\equiv 1.81$ eV, $T_0=300$ K, $c=1$ J/g K, $\rho=1$ g/cm^3. For these numbers, the dimensionless units are: time 10 ns, temperature 300 K, length 0.1 μm, intensity 300 kW/cm^2, fluence 3 mJ/cm^2. Such parameters are typical for excimer-laser ablation of strongly absorbing polymers.

zero derivative there. The number of broken bonds below the surface is very close to n_{cr}. After the onset of ablation the concentration n_b (in the laboratory frame) continues to increase. As a result, the interface (its position h is determined by the condition $n_b(h)=n_{cr}$) propagates explosively. The velocity has a singularity $v\propto(t-t_{cr})^{-1/2}$ near ϕ_{th} (Fig. 2). In reality v is restricted by physical constrains, e.g., by the sound velocity.

For the case depicted in Fig. 2, the surface temperature T_s increases before the onset of ablation. Using the saddle-point method (fastest reaction just before t_{cr}), one obtains from Eq. (3.6):

$$b_{cr}=\int_0^{t_{cr}} k_s(t)\,dt \approx k_s \left.\frac{T_s^2}{T_a \dot{T}_s}\right|_{t=t_{cr}},$$

$$A\approx\left(\frac{T_a\dot{T}_s}{T_s^2}\right)^{1/2} l_k\Bigg|_{t=t_{cr}} = \left(\frac{2D_s}{\alpha I_s/c_s\,\rho\dot{T}_s-1}\right)^{1/2}\Bigg|_{t=t_{cr}} \qquad (3.7)$$

The second equality for A was obtained by using Eq. (3.3) for l_k and Eq. (3.4). A is equal to infinity if heat conduction is neglected. With heat conduction, t_{cr} increases while A decreases. A depends *explicitly* on the profile and duration of the laser pulse and *implicitly* on k_0 and T_a, via t_{cr}. For constant parameters, $T_s(t)$ is known [1], and t_{cr} can be estimated from Eq. (3.7).

3.1. Surface temperature

After the ablation onset, T_s will increase slower, or even decrease, due to the movement of the ablation front. The Green function of the (linear) heat Eq. (2.1) can be obtained for *arbitrary* $v(t)\equiv\partial h/\partial t$. Its Taylor expansion for small h yields for the surface temperature

$$T_s\approx T_s(h\equiv 0)+\frac{h^2}{2}\frac{\partial^2 T}{\partial x^2}(h\equiv 0,\ x=0,\ t=t_{cr}) \qquad (3.8)$$

$T(h\equiv 0)$ refers to the case without movement. Thus, near ϕ_{th}, changes in T_s are only due to changes in the position of the front in the laboratory frame—the interface penetrates the temperature distribution created *before* ablation. With h from Eq. (3.6), (3.8) predicts a jump in the time derivative $\dot{T}_s$. With $\partial^2 T/\partial x^2$ from Eq. (3.4) and A from Eq. (3.7) the *resulting* time derivative is equal to zero, i.e., $T_s\approx$ constant in Eq. (3.8). This shows why T_s quickly stabilizes (Fig. 2). It has the tendency to remain constant even for $I(t)\neq$ constant.

4. Near threshold behavior for short pulses

Broken bonds are accumulated during the time when the material is hot. With $\phi\approx\phi_{th}$, ablation starts *after* the laser pulse and also *after* the maximum temperature T_m is reached (Fig. 3). Consideration similar to that leading to Eq. (3.6), yields for the *total* ablated depth per pulse $h(t=\infty)$.

$$h(\infty)\approx\left[\frac{\Delta b}{b_{cr}}\right]^{1/2} l_k(t_m),\quad b_{cr}=\int_0^{t_{cr}} k_s(t)\,dt,$$

$$\Delta b=\int_{t_{cr}}^{\infty} k_s(t)\,dt \qquad (4.1)$$

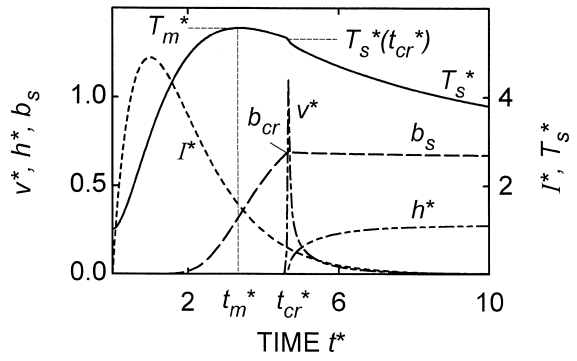

Fig. 3. Near threshold ablation for smooth laser pulse $I(t) = I_0 t/\tau \exp(-t/\tau)$. Ablation occurs *after* the pulse and *after* the maximal surface temperature T_m^* was reached at t_m^*; $\phi^* = 13.3$. The other parameters and notations are the same as in Fig. 2.

This allows the following interpretation. The profile $b(x)$, which is parabolic near $x = 0$

$$b(x) \approx (b_{cr} + \Delta b)\left(1 - x^2/l_k^2(t_m)\right) \tag{4.2}$$

is created mainly at $t \approx t_m$ when the reaction rate has a sharp maximum. Afterwards, all material with $b(x) > b_{cr}$ is ablated. In reality, of course, $b_s \le b_{cr}$ at any moment. To relate $h(\infty)$ to the parameters of the laser pulse, we note, that *near the threshold*, the influence of ablation on the evolution of the temperature (and reaction rate in Eq. (4.1)) can be neglected. This allows to combine two integrals in Eq. (4.1) and to apply the saddle point method near t_m:

$$b_{cr} + \Delta b = \int_0^\infty k_s(t)\,dt \approx \left[\left(\frac{2\pi T_s^2}{-\ddot{T}_s T_a}\right)^{1/2} k_s\right]\Bigg|_{t=t_m} \tag{4.3}$$

At threshold one should set $\Delta b = 0$ and find the temperature at $t = t_m$. As $h(\infty) \propto \Delta b^{1/2}$ in Eq. (4.1), h has a square-root dependence on ϕ near ϕ_{th}. With constant parameters, and $T_0 \ll T_m$

$$h(\infty) \approx \frac{1}{\alpha}\left[\frac{2\theta_m I_0}{I_m}\right]^{1/2}\left(\frac{\phi - \phi_{th}}{\phi_{th}}\right)^{1/2},$$

$$\phi_{th} \approx \frac{c\rho T_a}{A_s \alpha}\left[\frac{\tau^*}{\theta_m \ln\left[y/\sqrt{\ln y}\right]}\right],$$

$$y = \frac{k_0}{b_{cr} D\alpha^2}\left[\frac{2\pi\theta_m}{-\ddot{\theta}_m}\right]^{1/2} \tag{4.4}$$

$\tau^* = D\alpha^2\tau$ is the dimensionless pulse duration, $\theta(t^*) \equiv I_0^{-1}\int_0^{t^*} e^{t^*-t_1^*}\,\mathrm{erfc}\sqrt{t^*-t_1^*}\,I(t_1^*)\,dt_1^*$ the dimensionless temperature, and A_s the absorptivity. I_0 and τ are defined in such a way that $\phi = I_0\tau$. The expressions in square brackets can be calculated for a given temporal profile of the pulse.

5. Depletion of species and real ablation

The main conclusion of the preceding discussion is that volume degradation results in a *sharp* onset of ablation. This is in contrast to the behavior expected for a purely surface process. Ablation of polymers reveals also an Arrhenius tail in *mass loss* measurements near ϕ_{th} [12]. This does not contradict the present model, as the preceding discussion refers to a layer by layer material removal and *crater formation*, revealed in *profile* measurements. In a previous paper [17], we considered two *different* processes: the creation of volatile species and their depletion from the *volume*, and *surface* ablation. Within the present picture, *both* processes result from *the same* bulk reaction. It breaks the bonds, destroys polymer chains, and simultaneously creates trapped volatile species. For example with polyimide (PI), these are mainly CO molecules [18] cleaved from imide rings [19] which leads to carbonization of the material and a second threshold in multiple-pulse ablation [20]. Typical activation energies for the degradation of PI are about 1.5 eV [21], which are in agreement with the analysis of ablation data [8,9,14].

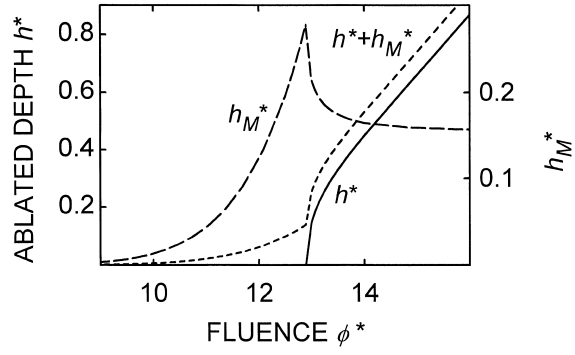

Fig. 4. Real ablated depth h (solid line), h_M (dashed line) related to mass loss due to depletion, M, and the total effective 'depth' $h_M + h$ (dotted line). $m_v/m_t = 0.5$. The laser parameters are the same as in Fig. 3, and the other parameters as in Fig. 2.

With $\phi < \phi_{th}$, *all* volatile species result in a mass loss. As the number of broken bonds obeys (2.2), this results in an Arrhenius tail. With $\phi > \phi_{th}$, volatile species leave the material *together* with the ablation products. When ablation ceases ($n_b(x=0) < n_{cr}$) some of the volatile species still exist below the surface and leave the material afterwards. This results in an additional mass loss, M (per unit area), which does *not* contribute to the ablated (crater) depth. M, which is due to the depletion of species, is proportional to the number of broken bonds *left within the material after ablation*, i.e., at time $t = t_{end\ of\ ablation}$.

$$M = m_v N_0 \int_0^\infty n_b(x)\,dx,$$

$$h_M \equiv \frac{M}{\rho} = \frac{m_v}{m_t}\int_0^\infty n_b(x)\,dx, \qquad (5.1)$$

N_0 is the total concentration of virgin bonds, and m_v the mass of volatile products produced per broken bond. m_v/m_t is the mass fraction, related to volatile species (per bond). It depends on the chemistry of the process, but it is always less then one (for PI it is about 0.5 [19]). In previous investigations the ablated depth was calculated from the total mass loss $h\rho + M$. This is erroneous, because the depletion of species may take place without any change in the surface profile. In order to compare the predictions of the model with such measurements, we introduced the 'depth' h_M related to M, and also the *total* effective 'depth' $h + h_M$.

The dependence of h_M on fluence is shown in Fig. 4 by the dashed line. Below threshold, an Arrhenius-type behavior is found. At high fluences, h_M becomes almost constant; it has a sharp maximum near ϕ_{th}. This is because *above* threshold, the modified region ablates *together* with volatile species, which decreases their contribution to the depletion-related mass loss. An increase in surface modification around ϕ_{th} was observed in conductivity measurements [22].

The *total* effective ablated depth (dotted line) is monotonous with fluence, but may demonstrate an inflection point or singularity in slope. Such a behavior, reported, e.g., in Ref. [2] is inherent in the present model and does not require additional mechanisms related for example to the screening of the incoming radiation by ablated products.

6. Conclusions

It is shown, how *bulk photothermal* degradation of polymers by laser light may result in ablation. The model predicts a sharp ablation threshold and the differences in ablation rates measured by profilometry and mass loss. A similar description can be applied to other materials such as HTSC, oxidic (ferroelectric) perovskites, and other materials, where a depletion of species for fluences $\phi \le \phi_{th}$ is observed [1]. A direct comparison with the experimental results requires the consideration of the heat effect of bond breaking reaction, backward and/or subsequent chemical transformations, changes in material properties, screening of incoming radiation, etc. This is the prospect for further research.

Acknowledgements

This work was supported by the 'Fonds zur Förderung der Wissenschaftlichen Forschung in Österreich' and 'Russian Foundation for Basic Researches'.

References

[1] D. Bäuerle, Laser Processing and Chemistry, Springer, Berlin, 1996.
[2] R. Srinivasan, B. Braren, Chem. Rev. 89 (1989) 1303.
[3] R. Srinivasan, V. Mayne-Banton, Appl. Phys. Lett. 41 (1982) 576.
[4] S. Lazare, V. Granier, Laser. Chem. 10 (1989) 25.
[5] G.D. Mahan, H.S. Cole, Y.S. Liu, H.R. Philipp, Appl. Phys. Lett. 53 (24) (1988) 2377.
[6] B. Luk'yanchuk, N. Bityurin, S. Anisimov, D. Bäuerle, Appl. Phys. A 57 (1993) 367.
[7] G.C. D'Couto, S.V. Babu, J. Appl. Phys. 76 (5) (1994) 3052.
[8] N. Arnold, B. Luk'yanchuk, N. Bityurin, Appl. Surf. Sci. 127 (1998) 184.
[9] B. Luk'yanchuk, N. Bityurin, M. Himmelbauer, N. Arnold, Nucl. Instrum. Meth. B 122 (1997) 347.
[10] S.R. Cain, F.C. Burns, C.E. Otis, B. Braren, J. Appl. Phys. 72 (1992) 5172.
[11] S. Cain, J. Phys. Chem. 97 (1993) 7572.

[12] S. Küper, J. Brannon, K. Brannon, Appl. Phys. A 56 (1993) 43.
[13] F.C. Burns, S.R. Cain, J. Phys. D 29 (1996) 1349.
[14] K. Piglmayer, E. Arenholz, K. Ortwein, N. Arnold, D. Bäuerle, Appl. Phys. Lett. (1998).
[15] N. Bityurin, N. Arnold, B. Luk'yanchuk, D. Bäuerle, Appl. Surf. Sci. 127 (1998) 164.
[16] N. Arnold, N. Bityurin, D. Bäuerle, in preparation.
[17] M. Himmelbauer, N. Bityurin, B. Luk'yanchuk, N. Arnold, D. Bäuerle, Proc. SPIE 3093 (1997) 224.
[18] S. Lazare, W. Guan, D. Drilhole, Appl. Surf. Sci. 96–98 (1996) 605.
[19] R. Srinivasan, R.R. Hall, W.D. Loehle, W.D. Wilson, D.C. Allbee, J. Appl. Phys. 78 (1995) 4881.
[20] Z. Ball, T. Feurer, D.L. Callahan, R. Sauerbrey, Appl. Phys. A 62 (1996) 203.
[21] W.W. Wright, in: N. Grassie (Ed.), Developments in Polymer Degradation 3, Appl. Sci. Publisher, London, 1981.
[22] E. Arenholz, J. Heitz, M. Wagner, D. Bäuerle, H. Hibst, A. Hagemeyer, Appl. Surf. Sci. 69 (1993) 16.